This study considers a multistage thermoacoustic engine with an external heat supply, used to convert low-grade heat from solar and geothermal sources into electrical energy.

The study of improving the efficiency of thermoacoustic engines using low-grade heat sources remains unresolved because of high self-starting temperatures and significant heat loss. This study examines an approach based on the design of a multistage thermoacoustic engine with an external heat supply, which reduces the starting temperature and improves efficiency.

To achieve this goal, mathematical modeling was performed in the DeltaEC environment using a linear approximation of Rott equations; a laboratory prototype of an eight-stage engine was designed. The results showed that at a heater temperature of 105°C and an average pressure of 2 bar, an acoustic oscillation frequency of 64 Hz and an electrical power of up to 80 W are achieved with an efficiency of approximately 12%.

Distinctive features of the proposed structure include optimized stage and resonator geometry, the use of a traveling acoustic wave, as well as the ability to operate at low heating temperatures, which distinguishes it from existing analogs. It has been established that increasing the stage diameter to an optimal ratio of 10:1 relative to the resonator, improving thermal insulation, and increasing pressure to 8 bar could increase efficiency by up to 40%.

The practical significance of this work is its potential for implementing the designed engine in autonomous power supply systems in rural and remote areas of the Republic of Kazakhstan where electricity costs are traditionally higher and fuel delivery is difficult. The results confirm the feasibility of using thermoacoustic technologies for sustainable and environmentally friendly energy supply

Keywords: thermoacoustic engine; low-grade heat; autonomous power supply; energy efficiency; geothermal; Stirling engine

UDC 621.43

DOI: 10.15587/1729-4061.2025.341710

DESIGN OF AN ALTERNATIVE ENERGY SOURCE BASED ON A MULTISTAGE THERMOACOUSTIC ENGINE WITH EXTERNAL HEAT SUPPLY

Aliya Alkina
PhD, Senior Lecturer*
Yermek Sarsikeyev
PhD, Associate Professor
Department of Electrical Equipment Operating
S. Seifullin Kazakh Agrotechnical Research University
Zhenis ave., 62, Astana, Republic of Kazakhstan, 010000
Ali Mekhtiyev
PhD, Professor, Vice-Rector for Science and Innovation**
Yelena Neshina
Corresponding author
PhD, Associate Professor, Head of Department*
E-mail: 1_neg@mail.ru
Ruslan Mekhtiyev
Master of Science in Engineering, Engineer
Department of Automation and Production Processes**
*Department of Power Systems**
**Abylkas Saginov Karaganda Technical University
N. Nazarbayev ave., 56, Karaganda,
Republic of Kazakhstan, 100027

Received 30.07.2025
Received in revised form 29.09.2025
Accepted 07.10.2025
Published 30.10.2025

How to Cite: *Alkina, A., Sarsikeyev, Y., Mekhtiyev, A., Neshina, Y., Mekhtiyev, R. (2025). Design of an alternative energy source based on a multistage thermoacoustic engine with external heat supply. Eastern-European Journal of Enterprise Technologies, 5 (8 (137)), 28–37. https://doi.org/10.15587/1729-4061.2025.341710*

1. Introduction

There is no doubt that the development of renewable energy is relevant because the search for environmentally friendly energy sources could solve a number of problems associated with the growth of greenhouse gas emissions and environmental pollution from various waste. It is also necessary to consider the global trend of solar energy development, which is annually evolving in terms of generation efficiency, as well as the trend of decreasing the cost of electricity generated from renewable sources.

The Republic of Kazakhstan has historically relied on coal and other fossil fuels as the basis of its energy system. According to a UNCTAD report, the country is among the top 10 globally in terms of confirmed coal reserves – approximately 29.4 billion tons, which is ~2.4% of global reserves; at the current level of production, these resources can cover the country's needs for 200–300 years [1]. According to statistics for 2024, thermal power plants (TPPs) and combined heat and power plants (CHPs) generated approximately 63.2%.

At the same time, there are a number of unresolved issues regarding the high costs of operating renewable energy sources in the Republic of Kazakhstan. The lack of a balanced approach to renewable energy sources within the energy system, their dependence on natural conditions, and the need for energy storage pose certain challenges to achieving a complete transition to renewable energy sources by 2050. These circumstances call into question the feasibility of decarbonizing the economy and necessitate the search for new technologies and the improvement of existing ones.

The Republic of Kazakhstan has vast territories and ranks 9th in terms of area. This creates a number of problems with land development and cultivation. The lack of its own effective autonomous energy supply systems hinders the development of agriculture, particularly livestock farming, since the cost of energy in remote rural areas is 2–4 times

higher than for residents of large settlements [2]. This situation is caused by the significant length of networks and relatively high losses during energy transportation, as well as the presence of small private companies – intermediaries that increase the cost of energy for the end consumer. Another pressing issue in energy supply is the centralized power supply for rural settlements whose residents are engaged in growing vegetables and fruits as energy is required to operate the irrigation system of the fields. Currently, autonomous consumers mainly use diesel or gasoline electric generators, but the cost of electricity is even higher because investment in equipment and its operation is required.

Fuel delivery over distances of 100 to 500 km is a very expensive process [3]. Taking into account the accumulated global experience, as well as the development of renewable energy sources equipment and technologies, our paper proposes an improvement in the technology for designing a cogeneration energy source capable of converting solar radiation at high efficiency. The essence of the proposed solution is to use a thermoacoustic engine with external heat supply (TAE) and a solar collector with a heat accumulator. The proposed source could be used in autonomous (decentralized) energy supply systems in rural areas.

In the southern regions of Kazakhstan, the temperature almost never drops below 5°C, the duration of sunshine per year can be 2800–3000 hours or more. The radiated power can reach 1700–1800 kW per 1 m^2 per year, therefore, the use of a solar collector as a heat source is quite justified [4]. Moreover, its efficiency could reach 80–90% while its cost is much lower than that of photovoltaic plants.

Using a multi-stage TAE, it is possible to convert the energy of heated water into electric current. TAE has a relatively simple structure; it has no moving (rotating) parts other than the linear generator or a two-way turbine with a synchronous generator, ensuring a long service life. For stand-alone renewable energy sources based on TAEs, with a power of up to 1–3 kW, a linear generator could be used, but for higher power, this generator will be less efficient and more expensive. In the power range from 3 to 100 kW, when one or a group of consumers requires more power, the optimal solution is to use a two-way turbine connected to a rotating synchronous generator, which will be significantly more efficient than a linear generator.

In particular, the authors of [5] analyze the key obstacles to the development of renewable energy policy in Kazakhstan, including the lack of incentive mechanisms and the risks of investment uncertainty.

Thus, designing thermoacoustic generators based on low-grade heat is a relevant area. Such devices are necessary for the autonomous and environmentally friendly energy supply to remote and rural areas.

2. Literature review and problem statement

Papers [6, 7] demonstrate the dependence of Stirling engine efficiency on pressure and heat recovery. However, problems with leaks and heat loss remain. This is due to the inherent difficulties of operating piston systems at high pressures, making the relevant research unsuitable for use with low-grade heat sources. Those studies are relatively outdated but they contain the entire theoretical basis for the operation of TAE and examples of its successful practical application.

Modern research on thermoacoustic engines shows that the transition from piston systems to acoustic waves eliminates the key problems of friction and working fluid leakage [8]. However, unresolved issues remain related to low output power and the need for precise matching of resonator parameters. These difficulties could be overcome through multi-stage structures, as confirmed by recent research. Recent advances have been associated with the use of multi-stage designs and traveling waves: for example, in [9], an efficiency of up to 49% of the Carnot cycle was recorded, although scaling remains difficult.

Paper [10] reports the results from numerical modeling of a single-stage TAE with a closed resonator, demonstrating that the choice of geometry has a critical impact on the stability of the acoustic wave. However, questions remain regarding the practical implementation of these structures, as numerical models do not always adequately reflect real heat transfer and acoustic losses.

In [11], a four-stage TAE was designed, which operated at ~100°C but further implementation was limited by the high cost and complexity of the structure. This was a definite breakthrough in thermoacoustic; several prototypes were fabricated, but, like previous researchers, it was not possible to bring their development to industrial implementation. The use of four stages with a larger diameter than the resonator allowed the authors not only to reduce the start-up temperature, in comparison with a single-stage TAE, but also to shorten the resonator length.

Study [12] demonstrated the possibility of using a multi-stage thermoacoustic energy conversion system in autonomous power supply systems. It is shown that the use of low-grade heat from solar collectors and geothermal sources is a promising direction. The issues of increasing power and reducing the self-starting temperature remain, which requires additional research.

In [13], the principles of generating thermoacoustic waves in closed resonators are considered, focusing on standing waves and their interaction with heat exchange elements. However, the proposed structures are primarily theoretical in nature, and the work does not describe engineering solutions that enable long-term stability of the device under conditions of variable heat flux.

In [14], the possibility of improving the efficiency of thermoacoustic energy conversion through the use of non-standard resonator geometries is investigated. Despite this, the work does not consider the issues of thermal insulation and integration of such systems with real sources of low-grade heat, which significantly limits the applicability of the proposed approach.

In [15], the advantages of a traveling wave are demonstrated but an analysis of stability under long-term load is lacking. In [16], an algorithmic optimization of the output power of TAE was performed using the Nelder-Mead method, which made it possible to increase the electrical power at medium pressure. However, this approach is limited by the computational capabilities of the models and does not take into account real process losses.

In [17], the influence of the stack length on the efficiency of TAE is demonstrated: with TAE length of 6 cm, maximum efficiency is achieved. However, under actual conditions, maintaining the optimal stack length can be difficult due to instability of temperature regimes and mechanical limitations.

In [18], the results of modeling a three-stage TAE with a traveling wave were reported, which confirmed the advantages of this configuration over systems with a standing wave. However, the question of optimizing the resonator size

to increase power under autonomous power supply conditions remains open.

Paper [19] reports the results of modeling thermoacoustic processes using numerical methods, which made it possible to identify key patterns in the propagation of acoustic vibrations in multi-stage configurations. However, the model does not take into account the influence of design simplifications and heat losses in real devices, which complicates its use at the engineering design stage.

Paper [20] describes the development of compact thermoacoustic modules for autonomous power supply of low-power consumers. The authors demonstrate a high degree of miniaturization, but the device is designed for a stable temperature gradient, which makes it less suitable for conditions with variable solar or geothermal energy intensity.

Study [21] analyzes the scalability of thermoacoustic systems. At the same time, the work gives only conceptual proposals, not supported by experimental data or heat transfer models.

Paper [22] reports a model of a traveling-wave system for controlling heat flows in aircraft installations, demonstrating the feasibility of integrating a thermoacoustic system into actual heat transfer circuits to stabilize the thermal conditions of equipment.

In [23], a configuration of a thermoacoustic cooling system with a bypass circuit was proposed, which made it possible to significantly increase the efficiency of heat and mass transfer and reduce the energy consumption of the installation.

Our review of the literature reveals that, despite significant advances in thermoacoustic systems, key challenges limiting their practical application remain unresolved. These challenges include low output power and system efficiency, high self-starting temperatures, significant thermal and hydraulic losses in the resonator and regenerator, and the lack of comprehensive studies combining numerical modeling and experimental testing of multistage configurations. Furthermore, most existing models do not account for the influence of stage and diffuser geometry on acoustic wave stability and temperature gradient distribution when operating with low-grade heat sources (solar and geothermal). Engineering solutions to enable efficient engine operation at temperatures below 100°C remain insufficiently developed.

Thus, an unresolved scientific and technical challenge is to design a multistage thermoacoustic engine with an external heat supply that would reduce the self-starting temperature and increase the efficiency of converting low-grade heat into electrical energy.

3. The aim and objectives of the study

The objective of this study is to improve the efficiency of converting low-grade heat into electrical energy in a multistage thermoacoustic engine with external heat input by improving its structure. This could make it possible to design an alternative energy source for autonomous power supply systems for rural and remote consumers. This solution reduces dependence on diesel and coal-fired generators, lowers the cost of electricity, and ensures an environmentally friendly energy supply.

To achieve this aim, the following objectives were accomplished:

– to conduct an analytical and numerical study of the thermoacoustic Stirling engine;

– to propose a structure for a multistage low-temperature thermoacoustic engine with cylindrical stages, reducing the self-starting temperature and improving the efficiency of converting low-grade heat;

– to experimentally validate parameters of the designed eight-stage thermoacoustic Stirling engine.

4. Materials and research methods

The subject of our study is a multistage thermoacoustic engine with external heat input, designed to utilize low-grade heat from solar and geothermal systems.

Our hypothesis suggested that increasing the number of stages and optimizing the engine geometry would reduce the self-starting temperature to 60°C. This should also improve the system's efficiency when operating on low-grade heat sources, such as solar collectors and geothermal wells. As a result, such an engine could be effectively used in autonomous power supply systems.

To validate the model, experiments and calculations are being conducted using the DeltaEC linear thermoacoustic modeling platform (USA). The program is freely available at: https://doi.org/10.1016/j.apacoust.2021.108136.

DeltaEC performs numerical integration using a low-amplitude linear approximation technique based on the Rott equations. The program allows for calculations of the parameters of any thermoacoustic engine and numerical simulation of working fluid oscillation processes. This program was also used to calculate the stage and resonator parameters. An eight-stage thermoacoustic engine with a thermodynamic Stirling cycle similar to the Alpha type [6, 7] was chosen as the object of study.

The resonator length was determined using a well-known relationship from the physics of acoustics [12].

$$f = \frac{\nu}{\lambda}, \quad (1)$$

where ν is the speed of sound propagation,

λ is the wavelength of the sound wave.

Fig. 1 shows a photograph of a laboratory prototype of TAE.

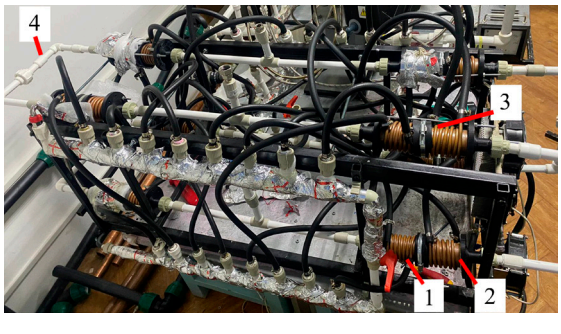

Fig. 1. Photograph of a laboratory prototype of a thermoacoustic Stirling engine: 1 — cold heat exchanger; 2 — hot heat exchanger; 3 — stage with heat exchangers and regenerator; 4 — tubular resonator

Atmospheric air is used as the working fluid. The designed TAE structure operates at a medium pressure, with a minimum of 2 bar and a maximum of 10 bar. The maximum working fluid pressure was approximately 2 bar. The design of TAE employed the theoretical foundations of thermody-

namics, acoustics, and mechanics, as well as existing mathematical models and expressions derived by authors whose papers are included in the list of references.

As part of the study, a proprietary computational model was built as a computer program implemented in Microsoft Office Excel (USA). Its algorithm includes formulas derived from the fundamental laws of ideal gas thermodynamics. This approach implies certain assumptions: the working fluid is treated as an ideal gas, and the temperatures of the hot and cold TAEs are assumed to be constant during engine operation. The regenerator divides the stage precisely at the center into two parts – hot and cold. Corrections for deviations in the adiabatic process were intentionally excluded from the model as their impact on the output power is minimal. The calculated TAE model is close in its characteristics to existing analogs based on a developed software application that allows the system to take into account dead gas volume. The necessary parameters for system evaluation are the energy for a full cycle, the power generated at fixed angular velocity values, as well as the pressure generated by the working fluid, with the corresponding units of measurement: J, W, and bar.

The program automatically converts values to SI units. The average temperature in the regenerator is calculated using the Schmidt method. The program plots a PV graph, which represents the relationship between pressure and gas volume. One of the engineering challenges was determining the key parameter – acoustic pressure over time. For this purpose, a Sound Card Oszilloscope microphone (Germany) was placed in the resonator cavity, used as an oscilloscope with two measurement channels. Special software was developed to record the amplitude and frequency of acoustic vibrations over time in the range from 20 Hz to 20 kHz.

To monitor TAE parameters, an integrated control system (ICS) was specially designed to display changes in pressure, acoustic power, and temperature. The ICS is based on an Arduino microcontroller, optical and analog sensors, and actuators (relays). The system is designed to collect and process data from DS18B20 digital temperature sensors, an analog pressure sensor, and a ZS-V05 industrial microphone (China). The resulting data is displayed on a local LCD display and transmitted via a serial interface as CSV strings for subsequent visualization using Python software implemented with the PyQt6 and PyQtGraph libraries. The Arduino (USA) software utilizes the OneWire library for interacting with DS18B20 digital temperature sensors, as well as DallasTemperature, which implements a high-level protocol for working with these sensors. The sensors are connected to a bus organized on pin 2, allowing simultaneous measurements of up to four devices. Fig. 2, 3 show the external appearance of ISC; the data was displayed on the LCD display.

A 20 × 4 LCD display with an I^2C interface provides local representation of information. It displays both measured values (temperature, pressure, and noise level) and set relay control thresholds. This allows the operator to quickly assess the current system status and take appropriate action.

The local LCD display (20 × 4) is used to visualize current measurements:

– the first and second lines display measured temperatures from sensors (T1–T4);

– the third line displays pressure and noise level data;

– the fourth line displays set thresholds for the heater and chiller.

Fig. 2. Front panel of the integrated control system

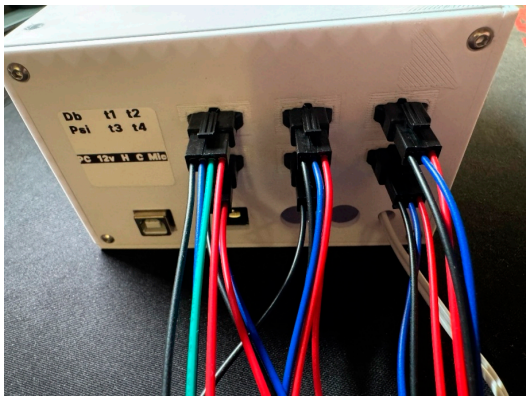

Fig. 3. Rear panel of the integrated control system

In addition to temperature sensors, the system reads analog values from a pressure sensor connected to connector A0 and a ZS-V05 noise sensor connected to connector A1. Pressure is calculated using an empirically established formula, where a voltage corresponding to 0.5 V is interpreted as 0 psi, and 4.5 V as 100 psi. Similarly, the microphone's analog signal is converted to a level scale from 30 to 200 dB (with a gain of 18 dB/V), which matches the sensor's specifications.

This provides the operator with a clear overview of the current system state, as well as the parameters used to control the actuators.

Developed using PyQt6 and PyQtGraph, the Python program provides the following functions:

– real-time monitoring: reading data from the Arduino via the serial port at 100 ms intervals. The program accepts CSV strings containing temperature, pressure, and noise level values;

– data visualization: data is stored in time-limited buffers (3 minutes, corresponding to 1800 points at 100 ms intervals) and displayed on separate plots for temperature, pressure, and noise;

– digital indicators: the interface displays the current values of measured parameters, as well as the unique serial numbers of the sensors obtained via the address discovery command;

– threshold management and reset: the user can set new thresholds for the heater and chiller using input fields (DoubleSpinBox) and the "Set Thresholds" button. A button for sending the "R\n" command to reset the Arduino is also provided.

– updating sensor addresses: the "Update sensor addresses" command sends the "D\n" command to the Arduino. The

program then waits for a string of addresses, and the digital indicators are updated to display the new values.

In addition to regularly collecting measurements, the Arduino receives commands via Serial. The "D\n" command initiates the detection of the addresses of the connected DS18B20 sensors. In the discoverSensors() function, all sensors are iterated through using the getAddress() method, after which a string containing the last 4 bytes of each address in hexadecimal format is generated and sent back to the interface. Thus, the unique serial numbers of the sensors are displayed on the digital indicators on the LCD and in the Python software module.

A relay was used to control the heater and chiller; heating and cooling were performed automatically based on the set temperature.

The actuators – SSR relays used to control the heater and chiller – switch the load based on the measured temperature. Control is provided via the microcontroller's digital pins. To improve operational stability, hysteresis logic has been implemented, preventing frequent relay switching at critical temperature levels.

Fig. 4 shows the DS18B20 temperature sensors used as an example.

The system designed integrates hardware components (DS18B20, analog pressure sensor, ZS-V05 noise sensor, relay, and LCD display) with intelligent software implemented in Arduino and Python. The software suite enables real-time data collection, processing, and visualization, supports threshold management for actuators, and automatic detection of unique sensor serial numbers. The use of hysteresis in the control logic enables a stable thermostatic mode, minimizing frequent relay switching under boundary conditions.

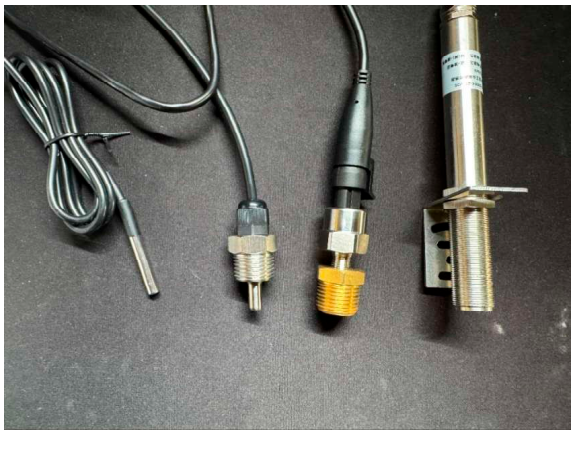

Fig. 4. General view of temperature sensors

5. Results of designing an alternative energy source based on a multistage thermoacoustic engine

5. 1. Analytical and numerical study of a thermoacoustic Stirling engine

To evaluate the theoretical solutions and calculations, a laboratory prototype of a multistage low-temperature TAE with cylindrical stages was specifically designed and built. The proposed TAE is similar to the four-stage engine design previously proposed by De Block of Aster Thermoacoustics and improved in 2010 by adding a ring resonator.

For the considered TAE design, calculations showed that the effective operating frequency is in the range of 50–65 Hz. The total length of the resonator and stages is 5.532 m, which ensures an oscillation frequency of 62 Hz; a slight frequency change of 5 Hz is possible at heating [12]. The oscillation frequency of the working fluid, obtained by calculation, is shown in the plot in Fig. 5.

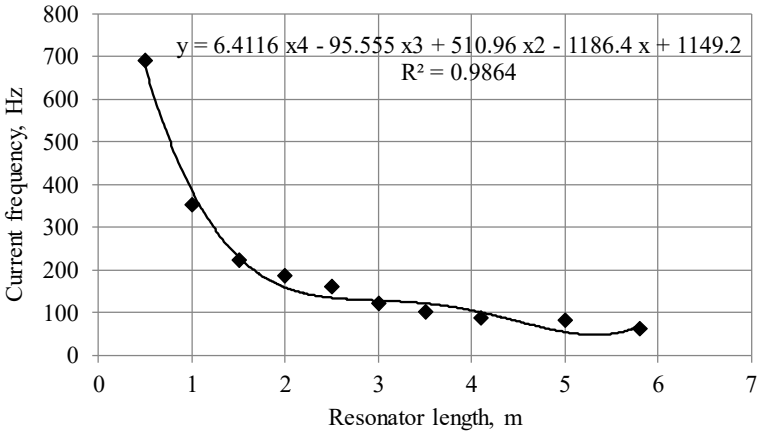

Fig. 5. Dependence plot of oscillation frequency on resonator length

Since a would-be alternative energy source based on a multi-stage thermoacoustic engine with an external heat supply will operate at a heater temperature of 60 to 110°C, it must be designed with more than four stages. A multi-stage low-temperature TAE with cylindrical stages is capable of converting low-grade heat from heated water from a solar collector or geothermal well into electric current with greater efficiency than Peltier thermoelectric converter elements, whose efficiency typically does not exceed 10%.

5. 2. Conceptual solution and design scheme of a multi-stage low-temperature thermoacoustic Stirling engine

The structure is based on well-known four-stage De Block configurations, improved to reduce hydraulic losses and self-starting temperatures. Our schematic describes the design principles, the interconnection of the stages, the resonator, and the diffusers, as well as the structural features of the heat exchange system.

The annular resonator is made of a plastic pipe with a diameter of 20 mm and an inner diameter of 12 mm. The resonator is connected to the stage using threaded couplings 1 with seals. Each stage has two couplings, one on each end face. The proposed TAE can operate at a working fluid pressure of up to 10 atm. To reduce hydraulic resistance and turbulence of the gas (working fluid) flow from the stage to the resonator and back, two diffusers 2 are used. The active section of each diffuser is 50 mm long and the diameter ratio is 12 to 60 mm. The internal diameter of the stage is 60 mm. Fig. 6 shows a schematic model of the stage, which contains two cylindrical heat exchangers (positions 3 and 5) and a resonator (position 4) located between them. Parts of the stage body were manufactured using 3D printing, including threaded coupling 1 and diffuser 2, as well as regenerator body 4.

When transitioning from the hot to the cold zone, the working fluid passes through regenerator 4, which accumulates some of the thermal energy. This allows partially cooled gas to enter the cold heat exchanger. During the return flow – from the cold to the hot heat exchanger – the

regenerator transfers the accumulated heat to the working fluid, which corresponds to the principle of the Stirling heat cycle. The cross-sectional area of both the cold (indicated by number 3) and hot (indicated by number 5) heat exchangers is 2921 mm^2.

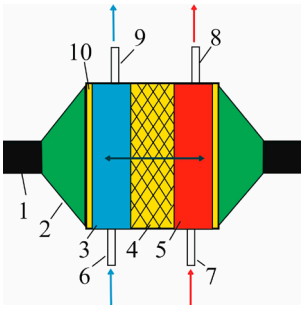

Fig. 6. Schematic diagram of a stage with two cylindrical heat exchangers: 1 — threaded connection; 2 — diffuser for the transition of the working fluid to the resonator and back to the stage; 3 — cylindrical copper heat exchanger of the cooling circuit; 4 — wire porous regenerator; 5 — cylindrical copper heat exchangers of the heating circuit; 6 — supply of the working fluid from the cold circuit; 7 — supply of the working fluid from the hot circuit; 8 — outlet of the working fluid to the hot circuit; 9 — outlet of the working fluid to the cold circuit; 10 — transition space from the diffuser to a heat exchanger

The cross-sectional area of the regenerator is 2640.74 mm^2 with an internal diameter of 58 mm. The ratio of the internal diameters of the heat exchanger and the resonator is 60/12 = 5, meaning the stage is 5 times larger in internal diameter than the resonator. De Block and other researchers found this ratio to be in the range of 12 to 20, but this was for a resonator diameter of 100 mm or more for four-stage TAEs. For eight-stage TAEs, the optimal ratio is 1:5, with each stage being five times larger in diameter than the resonator. The volumetric porosity of heat exchangers is 0.9 mm, and that of the resonator is 0.5 mm. Therefore, in the proposed structure, 50 mm is allocated to heat exchangers and 60 mm to the regenerator. This is confirmed by recommendations from [24].

Heat exchangers 3 and 4 are made of seamless, solid-drawn copper tubing with a diameter of 64 mm and a wall thickness of 1.5 mm. The length of the active portion of heat exchangers 3 and 5 is 50 mm. Regenerator 4 is made of copper wire and placed in a plastic casing for thermal insulation between heat exchangers 3 and 5. Coolant is supplied to cold heat exchanger 3 through inlet pipe 6 and leaves the heat exchanger through outlet pipe 9. A small intermediate cavity 10 with a depth of approximately 2–3 mm is provided between the diffuser and the heat exchanger. This represents the dead volume of the cold and hot heat exchangers. The cold heat exchanger is made of copper tubing with a 6 mm diameter copper tube wound onto its outer surface, providing circulation of the cooling heat carrier (automotive antifreeze). The fluid is moved by a pump, which maintains forced circulation.

Fig. 7 shows the end of the cold heat exchanger. Fluid enters the heat exchanger through port 4 and exits through port 5. This heat exchanger is connected to the cooling system via rubber hoses. The working fluid circulates in heat exchanger 3, transferring its heat to the coolant.

Fig. 8 shows a cross-section of a hot heat exchanger whose design is similar to the cold heat exchanger and differs in the presence of an outer casing that encloses a coil of copper tube 1 wound around a section of copper tube 2. Heated heat carrier (automotive antifreeze) circulates through copper tube 1. Tubes 1 and 2 are made of copper for improved heat transfer; that also applies to heat exchanger 3. The distance between the plates does not exceed 1 mm.

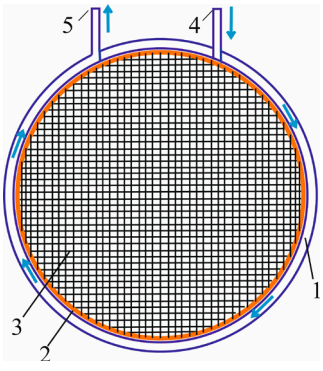

Fig. 7. Cold heat exchanger in cross-section: 1 — copper tube with a diameter of 6 mm; 2 — copper tube with a diameter of 64 mm; 3 — copper plates of heat exchanger; 4 — inlet pipe; 5 — outlet pipe

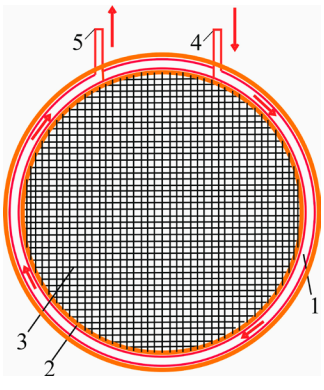

Fig. 8. Hot heat exchanger in cross-section: 1 — copper tube with a diameter of 6 mm; 2 — copper tube with a diameter of 64 mm; 3 — copper plates of heat exchanger; 4 — inlet pipe; 5 — outlet pipe

Fig. 9 shows a schematic diagram of an eight-stage TAE.

All stages are connected to both the heating and cooling systems. The TAE includes a heat carrier heating circuit, in which the liquid heat carrier is heated to 110°C at the location of acoustic sensor 1, after which it is distributed through pipelines to all hot heat exchangers 3. The system consists of eight pairs of identical heat exchangers. Each pair includes a cold and a hot heat exchanger, each connected to its own hot and cold circuits, which do not intersect. That is, the cold circuit connects the cylindrical copper heat exchangers of the heating circuit (shown in diagram 4) and the cylindrical copper heat exchangers of the cooling circuit (shown as number 2), as well as the supply (shown as number 10) and return (shown as number 11) pipelines of the cold circuit.

The Stirling cycle for this unit implies the following sequence:

1) heating of the working fluid in the form of air in the hot heat exchanger 3,

2) expansion in regenerator 5,

3) compression in the cylindrical copper heat exchanger of the heating circuit 4 as a result of partial cooling.

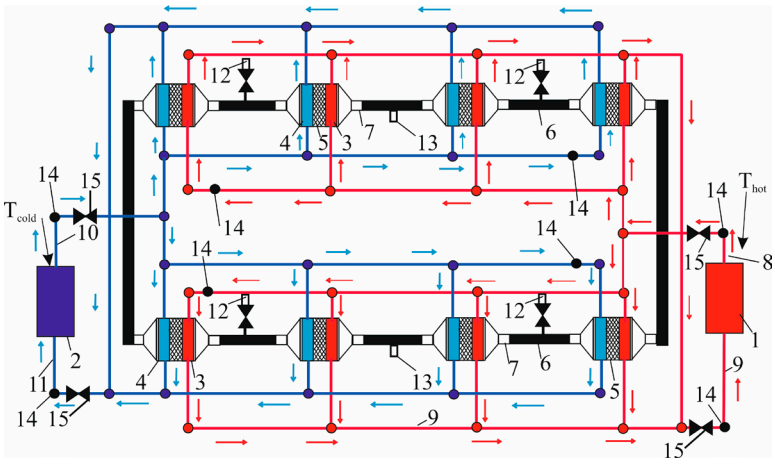

Fig. 9. Schematic diagram of thermoacoustic Stirling: 1 — heating system; 2 — cooling system; 3 — cylindrical copper heat exchanger of the heating circuit; 4 — cylindrical copper heat exchanger of the cooling circuit; 5 — wire regenerator; 6 — resonator chamber; 7 — coupling with seal; 8 — feed pipe of the heat carrier heating system; 9 — return pipe of the heat carrier heating system; 10 — feed pipe of the heat carrier cooling system; 11 — return pipe of the heat carrier cooling system; 12 — installation location of the pressure sensor; 13 — installation location of the acoustic sensor; 14 — installation location of the temperature sensor; 15 — shut-off valve

All stages are connected via a tubular resonator 6 and threaded couplings with seals 7. The heating system must be airtight; if the seal is broken, the pressure drops sharply and power is lost. Therefore, it is crucial to ensure a tight connection between the stages and the resonator. A traveling acoustic wave propagates through the resonators. The heating system has a supply line 8, through which the heated heat carrier (automotive antifreeze) enters the inlet of the hot heat exchanger 3. Return line 9 is connected to the outlet of this heat exchanger, carrying the cooled antifreeze back to the heater for reheating. The heating cycle is constantly repeated. The cooling system operates similarly but now circulates a cold heat carrier (automotive antifreeze). Supply pipe 10 delivers the cooled heat carrier to the inlet of cold heat exchanger 4. After passing through the heat exchanger, the heat carrier is heated, absorbing thermal energy, and returned through return pipe 11 to the cooling circuit, where it is cooled again before being fed back. The cycle is repeated and is continuous. Return pipe 12 of the heat carrier cooling system is used to control acoustic power. Return pipe 13 of the heat carrier heating system is used to control pressure. Eight temperature sensors 14 are installed to monitor the heat carrier temperature. Heating system 15 is used to shut off the supply and return pipes.

5. 3. Experimental verification of parameters for the designed eight-stage thermoacoustic Stirling engine

The results of our study showed that as the heater temperature increases from 60 to 105°C, the acoustic wave oscillation frequency increases within the range of 60 to 64 Hz, as shown in Fig. 10. It was established that the increase in oscillation frequency is associated with an increase in the temperature of hot heat exchangers. As the heater temperature increases, the average air temperature inside the TAE resonators increases, leading to an increase in the speed of sound within the resonator cavity and stages.

Fig. 11 shows a dependence plot for heating the working fluid to a temperature of 105°C as a function of time. The maximum temperature was reached in approximately 15 minutes.

Experimental data showed that the unit's output power is directly proportional to the area of the heat-exchange surfaces of the hot and cold circuits [6, 7]. The highest recorded power was 80 W at a working fluid temperature of 105°C and an acoustic wave frequency of approximately 64 Hz.

Fig. 12 shows a dependence plot of the thermoacoustic Stirling unit's power increase on the working fluid temperature.

Fig. 13 shows a plot constructed by theoretically calculating the efficiency, which directly depends on the output power of TAE.

The plot shows a relationship in which an increase in power is accompanied by an increase in efficiency values.

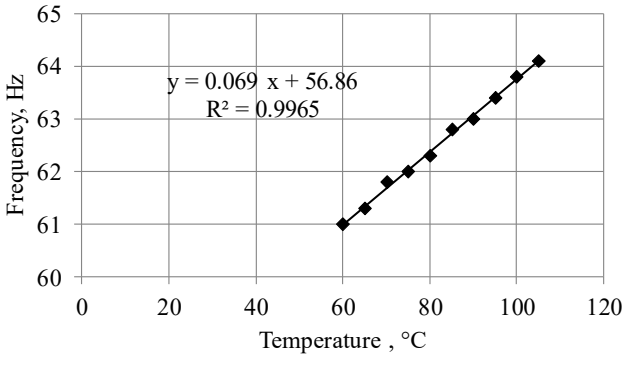

Fig. 10. Dependence plot of change in oscillation frequency on the increase in the temperature of the working fluid

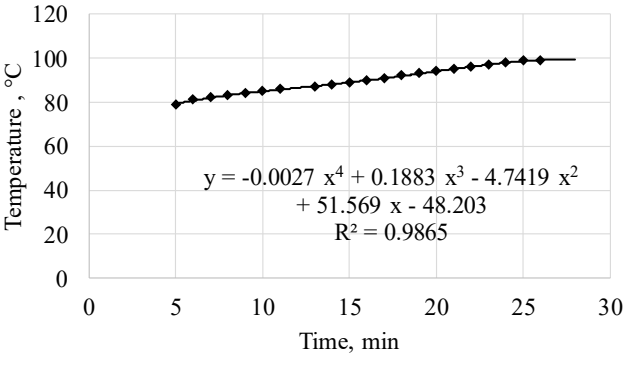

Fig. 11. Dependence plot of the temperature increase of the working fluid on time

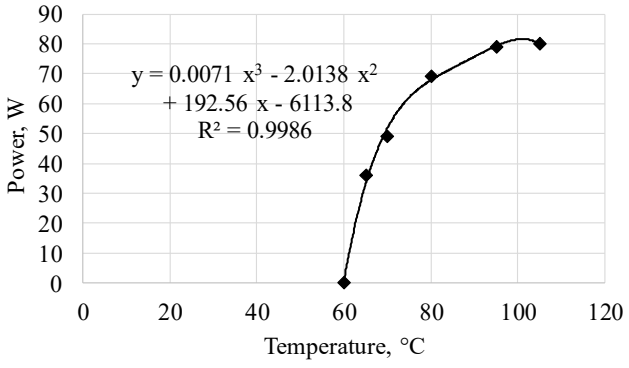

Fig. 12. Dependence plot of the increase in power of a thermoacoustic Stirling on the temperature of the working fluid

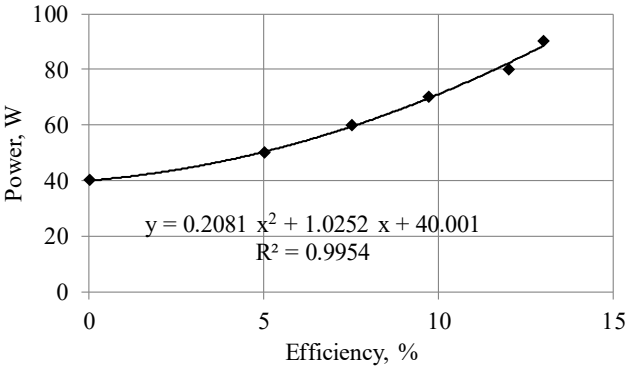

Fig. 13. Dependence plot of the increase in efficiency on the increase in output power

6. Results of designing a multi-stage low-temperature thermoacoustic Stirling: discussion

An increase in the acoustic oscillation frequency is observed as the heater temperature increases from 60 to 105°C. The frequency increases from approximately 60 to 64 Hz, which is due to an increase in the average working fluid temperature and the speed of sound in the resonator. This relationship is shown on the frequency-temperature and temperature-time plots (Fig. 10, 11). This relationship is consistent with the calculated operating frequency estimate obtained using the resonator length formula specified in Chapter 4. The chosen resonator section length is 5.532 m, yielding a calculated frequency of approximately 62 Hz (Fig. 5). The proportional increase in output power during heating is explained by an increase in the thermal drop across the heat exchangers (Fig. 12). An increase in temperature increases the acoustic power generated in the thermoacoustic engine circuit. This is further supported by the observed dependence of power on heat exchangers' area. The plot of efficiency growth versus output power shows a clear correlation between an increase in the number of connected tanks and an increase in excess energy consumption. When connecting a second tank, excess consumption increases more than fourfold compared to a single tank, indicating the need to optimize the system configuration to reduce energy losses.

It is consistent with the fundamental principles of Stirling engine operation outlined in [1, 2]. The theoretically calculated and experimentally confirmed efficiency of approximately 12% at 105°C and ~64 Hz (Fig. 13) is explained by a combination of structural factors in the current design: limited heat exchanger area, incomplete thermal insulation, and increased hydraulic losses due to the 5:1 stage-to-resonator diameter ratio, which reduces the effective acoustic power.

Unlike classic piston Stirling systems [6, 7], the elimination of friction pairs and seals through the use of an acoustic wave [8] eliminates the critical issues of leakage and service life for low-grade heat. Compared to single-stage configurations and closed-resonator models [10], the implemented multistage architecture and traveling wave (Fig. 6–9) reduce the self-starting temperature and increase efficiency. The proposed structure differs from the well-known four-stage setup [11] by the targeted optimization of the stage/resonator geometry to further reduce the self-starting temperature and operate with low-potential sources (solar collectors, geothermal wells at 70–80°C).

The limitations of our study include the following:

– low efficiency (≈12%) at the current stage of experiments;

– use of only atmospheric air as the working fluid;

– laboratory-scale setup.

A limitation of the study is that the experiments were conducted under stable laboratory conditions without taking into account dynamic operating factors (heat source temperature fluctuations, pressure variations, and environmental influences).

In the future, pilot tests are planned, connecting the setup to solar collectors and geothermal wells with seasonal fluctuation modeling. This work will focus on comprehensive design optimization, including stage geometry, the resonator, and diffusers, increasing operating pressure, improving thermal insulation, and using more efficient regenerators. Additionally, our plan includes testing the engine's integration with real low-grade heat sources in autonomous power systems and power scaling. Implementation of these measures could increase the efficiency to 40% and enable the widespread use of thermoacoustic setups for sustainable energy supply in remote and rural areas.

7. Conclusions

1. Based on analytical and numerical modeling, the effective operating frequency of a multistage thermoacoustic engine was determined to be 50–65 Hz with a total resonator length of 5.532 m, which corresponds to a calculated frequency of ≈62 Hz. The selected geometric parameters of the stages and resonator were confirmed to be correct, ensuring stable acoustic wave formation at heating temperatures ranging from 60 to 110°C. Our analysis revealed that the multistage architecture reduces the self-starting temperature and increases the efficiency of low-grade heat conversion compared to single-stage systems.

2. A conceptual and schematic solution for an eight-stage low-temperature thermoacoustic Stirling engine with cylindrical stages and a ring resonator has been proposed. The optimal ratio of the stage and resonator diameters, 5:1, was determined, enabling stable propagation of the traveling wave and reducing hydraulic losses. The concept includes operation at pressures up to 10 bar, improved thermal insulation, and the ability to integrate with solar and geothermal heat sources. It was found that reducing the resonator diameter and optimizing the heat exchange elements improves energy conversion efficiency and lowers the self-starting temperature of the system.

3. An experimental test of the eight-stage thermoacoustic engine was conducted, confirming the agreement between the calculated and measured parameters for frequency (60–64 Hz)

and operating temperature range (60–105°C). It was found that increasing the heater temperature increases the acoustic oscillation frequency and output power, reaching up to 80 W at 105°C, confirming the effectiveness of the multistage architecture. An efficiency of approximately 12%, limited by the area of heat exchangers and pressure losses, was experimentally confirmed; it was shown that optimizing the geometry and increasing the operating pressure can increase efficiency. High tightness and stability of the engine operation during long-term testing were noted, demonstrating the design's potential for further semi-industrial applications.

Conflicts of interest

The authors declare that they have no conflicts of interest in relation to the current study, including financial, personal, authorship, or any other, that could affect the study, as well as the results reported in this paper.

Funding

This research was funded by the Science Committee of the Ministry of Science and Higher Education of the Republic of Kazakhstan (Grant No. AP19679083 ''Development of prototypes of alternative energy sources of cogeneration type to improve the efficiency of energy supply to autonomous consumers'').

Data availability

The data will be provided upon reasonable request.

Use of artificial intelligence

The authors confirm that they did not use artificial intelligence technologies when creating the current work.

References

1. Beisengazin, K. (2025). Coal Sector of Kazakhstan: Challenges and Opportunities for Decarbonizing the Economy. Integrated Policy Strategies and Regional Policy Coordination for Resilient, Green and Transformative Development: Supporting Selected Asian BRI Partner Countries to Achieve 2030 Sustainable Development Agenda. Available at: https://unctad.org/system/files/information-document/unda2030d26-kazakhstan-coal_en.pdf?
2. Smatayeva, A., Temerbulatova, Z., Kakizhanova, T. (2024). The Impact of Economic and Environmental Factors on the Consumption of Renewable Energy: The Case of Kazakhstan. Eurasian Journal of Economic and Business Studies, 68 (4), 61–75. https://doi.org/10.47703/ejebs.v68i4.443
3. Zhakiyev, N., Burkhanova, D., Nurkanat, A., Zhussipkaliyeva, S., Sospanova, A., Khamzina, A. (2025). Green energy in grey areas: The financial and policy challenges of Kazakhstan's energy transition. Energy Research & Social Science, 124, 104046. https://doi.org/10.1016/j.erss.2025.104046
4. Minazhova, S., Kurrat, M., Ongar, B., Georgiev, A. (2025). Deploying a rooftop PV panels in the southern regions of Kazakhstan. Energy, 320, 135205. https://doi.org/10.1016/j.energy.2025.135205
5. Mouraviev, N. (2021). Renewable energy in Kazakhstan: Challenges to policy and governance. Energy Policy, 149, 112051. https://doi.org/10.1016/j.enpol.2020.112051
6. Walker, G. (1980). Stirling Engines. Oxford: Clarendon Pres, 276. Available at: https://www.scribd.com/doc/45062130/Stirling-Engines-G-Walker-Oxford-1980-WW
7. Fit, W. C. (Ed.) (1980). Steam Stirling Engines You Can Build. Village Press Publications, 169. Available at: https://www.scribd.com/document/820789063/Steam-Stirling-Engines-You-Can-Build
8. Mekhtiyev, A. D., Sarsikeyev, Y. Zh., Yugay, V. V., Neshina, E. G., Alkina, A. D. (2021). Thermoacoustic engine as a low-power cogeneration energy source for autonomous consumer power supply. Eurasian Physical Technical Journal, 18 (12 (36)), 60–66. https://doi.org/10.31489/2021no2/60-66
9. Tijani, M. E. H., Spoelstra, S. (2011). A high performance thermoacoustic engine. Journal of Applied Physics, 110 (9). https://doi.org/10.1063/1.3658872
10. Kruse, A., Ruziewicz, A., Tajmar, M., Gnutek, Z. (2017). A numerical study of a looped-tube thermoacoustic engine with a single-stage for utilization of low-grade heat. Energy Conversion and Management, 149, 206–218. https://doi.org/10.1016/j.enconman.2017.07.010
11. de Blok, K. (2010). Novel 4-Stage Traveling Wave Thermoacoustic Power Generator. ASME 2010 3rd Joint US-European Fluids Engineering Summer Meeting collocated with 8th International Conference on Nanochannels, Microchannels, and Minichannels, 73–79. https://doi.org/10.1115/fedsm-icnmm2010-30527
12. Sarsikeyev, Y., Mekhtiyev, A., Neshina, Y., Alkina, A., Mekhtiyev, R., Sharipov, T. (2024). An Alternative Thermoacoustic Energy Source for Power Supply to Autonomous Consumers. International Journal on Energy Conversion (IRECON), 12 (5), 184. https://doi.org/10.15866/irecon.v12i5.24875
13. Kropachev, P. A., Mekhtiyev, A. D., Bulatbayev, F. N., Sarsikeyev, Y. Zh. (2021). Method of restoring pivot connections cast iron Bushings of heat engine with external heat supply. Metalurgija, 60 (3-4), 343–346. Available at: https://hrcak.srce.hr/file/372269
14. Nikonova, T., Zharkevich, O., Dandybaev, E., Baimuldin, M., Daich, L., Sichkarenko, A., Kotov, E. (2021). Developing a Measuring System for Monitoring the Thickness of the 6 m Wide HDPE/LDPE Polymer Geomembrane with Its Continuous Flow Using Automation Equipment. Applied Sciences, 11 (21), 10045. https://doi.org/10.3390/app112110045

15. Mekhtiyev, A., Breido, I., Buzyakov, R., Neshina, Y., Alkina, A. (2021). Development of low-pressure electric steam heater. Eastern-European Journal of Enterprise Technologies, 4 (8 (112)), 34–44. https://doi.org/10.15587/1729-4061.2021.237873
16. Huntingford, F., Kisha, W. (2022). Algorithmic optimisation of the electrical power output of a low-cost, multicore thermoacoustic engine with varying resonator pressure. Sustainable Energy Technologies and Assessments, 49, 101776. https://doi.org/10.1016/j.seta.2021.101776
17. Farikhah, I., Elsharkawy, E. A., Nuroso, H., Novita, M., Marlina, D., Rahmatunnisa, K. et al. (2021). Study of Stack Length on Efficiency of Thermoacoustic Engine. 2021 IEEE 3rd Eurasia Conference on IOT, Communication and Engineering (ECICE), 580–582. https://doi.org/10.1109/ecice52819.2021.9645691
18. Sun, D., Luo, K., Zhang, J., Yu, Y. S. W., Pan, H. (2021). A novel non-linear one-dimensional unsteady model for thermoacoustic engine and its application on a looped traveling-wave thermoacoustic engine. Applied Acoustics, 181, 108136. https://doi.org/10.1016/j.apacoust.2021.108136
19. Guk, S., Lee, J., Kim, J., Lee, M. (2025). Advances and Challenges in Thermoacoustic Network Modeling for Hydrogen and Ammonia Combustors. Energies, 18 (2), 346. https://doi.org/10.3390/en18020346
20. Korobko, V., Shevtsov, A., Serbin, S., Wen, H., Dzida, M. (2025). Experimental Study of a Phase-Change Thermoacoustic Engine for Maritime Waste Heat Recovery System. Polish Maritime Research, 32 (2), 84–93. https://doi.org/10.2478/pomr-2025-0023
21. Baccoli, R., Di Meglio, A., Fenu, A., Massarotti, N. (2025). Design and performance of a ThermoAcoustic Electric Generator powered by waste-heat based on linear and nonlinear modelling. Applied Thermal Engineering, 276, 126938. https://doi.org/10.1016/j.applthermaleng.2025.126938
22. Rodriguez, J., Dyson, R. W., Wernet, M. P., Leibach, R. J. (2025). Thermoacoustic Thermal Management for Electric Aircraft. NASA Technical Report. AIAA SciTech Forum. Available at: https://ntrs.nasa.gov/citations/20240015017
23. Xiao, L., Luo, K., Zhao, D., Wu, Z., Xu, J., Luo, E. (2024). A highly efficient heat-driven thermoacoustic cooling system: Detailed study. Energy, 293, 130610. https://doi.org/10.1016/j.energy.2024.130610
24. Farikhah, I., Elsharkawy, E. A., Nuroso, H., Novita, M., Marlina, D., Rahmatunnisa, K. et al. (2021). Study of Stack Length on Efficiency of Thermoacoustic Engine. 2021 IEEE 3rd Eurasia Conference on IOT, Communication and Engineering (ECICE), 580–582. https://doi.org/10.1109/ecice52819.2021.9645691